

Instrument Science Report WFC3 2011-08

The Photometric Performance of WFC3/IR: Temporal Stability Through Year 1

J. S. Kalirai, S. Deustua, A. Rajan, and A. Riess
February 25, 2011

ABSTRACT

We analyze multiple observations of four bright HST spectrophotometric standard stars obtained with WFC3/IR in order to establish the temporal stability of the instrument over its first 1.5 years of science operations. Observations of one or more of the four stars, P330E, GD 153, GD 71, and G191B2B were obtained at multiple dither positions near the center of the array, and in all 15 imaging filters. A number of different read out modes and subarray sizes were used to ensure that a very high signal-to-noise measurement of the star was obtained in each observation. The first data sets followed shortly after installation of WFC3 in HST in May 2009 and over two dozen epochs have been observed up to late 2010. Analysis of the over 1200 individual observations shows that point source photometry with WFC3/IR is temporally stable to more than 99%.

1. The Infrared Channel of WFC3

The infrared (IR) channel of WFC3 uses a high quantum efficiency 1k x 1k HgCdTe array, with phenomenal sensitivity between 900 and 1700 nm (see e.g., Kalirai et al. 2009). The IR array offers several advantages over conventional CCD detectors, and similar systems will be used in top-priority missions by NASA and ESA over the next decade. Unlike CCD detectors, the accumulated signal over an exposure can be read out non-destructively multiple times, which reduces the effective read-out noise and provides a very high dynamic range to measure both very bright and very faint objects in the same exposure. For example, a 0.91 second exposure on WFC3/IR can be read out 15 times in the smallest subarray, with each read out being just 0.061. At the opposite end, the SPARS200 readout sequence provides non-destructive reads ranging from 2.9 seconds in the first sample all the way to 2802.9 seconds in the 15th sample.

The non-destructive read out capabilities of IR arrays also provide very efficient cosmic-ray rejection by identifying the sample in which a given cosmic ray impacted the array and removing it

by comparing to adjacent samples. Over long time periods, IR arrays are expected to suffer much less degradation than CCD detectors such as the WFPC2 and ACS CCDs, both of which show significant signs of radiation damage. For example, a major effort has been underway at STScI to correct for charge transfer efficiency in these detectors, as described in Anderson & Bedin (2010), and significant effects have already been measured for the UVIS channel of WFC3. The IR array of WFC3 is expected to suffer minimal damage in this respect and also to suffer minimal degradation in quantum efficiency.

In this ISR, we analyze over 1200 individual observations of spectrophotometric standard stars that have been obtained with WFC3/IR during the time period following its installation in HST in May 2009 to mid-November 2010. These data were collected in calibration programs CAL11451 (SMOV4) and CAL11926 (Cycle 17) with the primary goal of establishing the absolute throughput of the instrument, and have already demonstrated that the sensitivity of WFC3/IR is above expectations based on thermal vacuum ground tests (see Kalirai et al. 2009). The present goal is to compare the observations of common stars observed at a similar location of the IR array over a 16 month baseline to establish the temporal stability of the instrument. In addition to monitoring any unexpected trends in the quantum efficiency or general degradation, these measurements can help characterize WFC3/IR's sensitivity to transient phenomena that vary over timescales ranging from less than a day to several years.

2. Observations from CAL11451 and CAL11926

There are two calibration programs on WFC3/IR that have imaged bright spectrophotometric standards with high signal-to-noise. The first is CAL11451, which targeted both the cool solar analogue P330E ($V = 13.00$, $H = 11.48$) and the hot white dwarf GD 153 ($V = 13.35$, $H = 14.19$). These observations were obtained over 4 epochs separated by 1 day, 1 week, and 1 month in SMOV4, and each star was observed at multiple dither positions ensuring a very high signal-to-noise detection in all 15 IR filters. The program took 8 orbits to execute (e.g., 1 orbit for each star at each epoch) from July 13 to Aug 13th 2009, and is reported in Kalirai et al. (2009).

Based on the analysis of the SMOV4 data, we designed a longer Cycle 17 calibration program to repeat observations of these two stars over a 1 year baseline, and also to add two additional white dwarf spectrophotometric standards – GD 71 ($V = 13.03$, $H = 13.86$) and G191B2B ($V = 11.77$, $H = 12.66$). These observations also benefit from knowledge of the on-orbit instrument throughput and therefore exposure times were adjusted to ensure maximizing the signal-to-noise for each target. Additionally, we included subsets of observations in each of the 64, 128, 256, and 512 pixel subarrays, and obtained full frame exposures to explore any unexpected trends with the choice of aperture. These observations again included multiple dithered exposures over a small region of the array near the center, and typically exposed all 15 filters at each epoch.

We summarize the imaging data of each of these four stars in Table 1.

Table 1: WFC3/IR SMOV4 and Cycle 17 Temporal Stability Observations

Target ^a	Epochs
P330E	2009-07-13, 2009-07-14, 2009-07-21, 2009-08-13, 2009-11-20, 2009-12-29, 2010-02-03, 2010-05-05, 2010-06-08, 2010-07-04, 2010-08-19, 2010-09-16
GD 153	2009-07-13, 2009-07-14, 2009-07-21, 2009-08-11, 2009-12-24, 2010-02-08, 2010-02-18, 2010-02-19, 2010-04-08, 2010-05-07, 2010-06-05, 2010-07-03, 2010-11-17
GD 71	2009-11-01, 2009-11-24, 2010-02-16, 2010-08-25, 2010-09-29
G191B2B	2010-01-05, 2010-08-09

^aAn incorrect gain setting in the phase II proposal for CAL11926 affected observations of P330E on 2009-09-30 and 2009-10-02 and GD 71 on 2009-10-01 and 2009-10-05, and so these are excluded from our analysis.

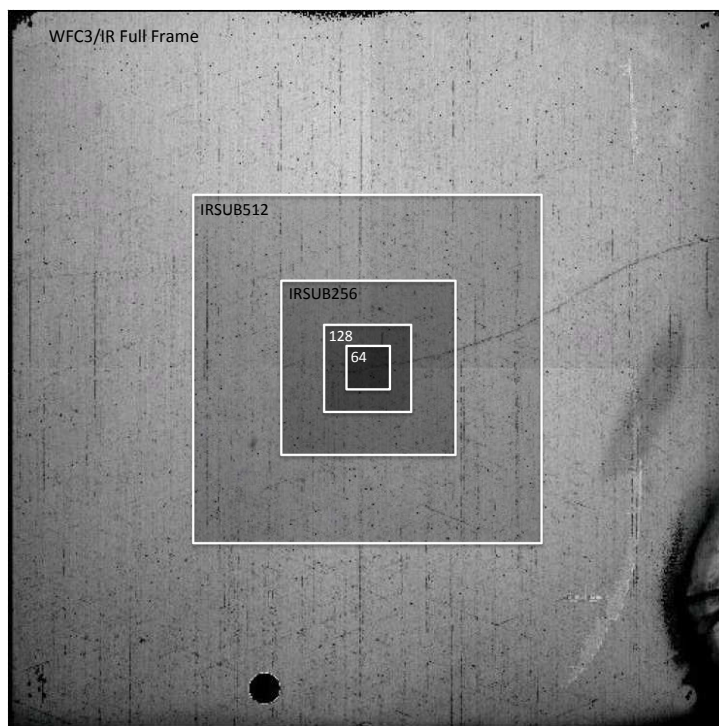


Fig. 1.— The location of the WFC3/IR subarrays on top of a full frame flat field image. Unlike the UVIS camera, the IR subarrays are centered in the field so all of our targets are imaged near the center of the array, but slightly shifted to avoid the intersection of the four quadrants.

3. Data Analysis and Photometry

We retrieved all data from CAL11451 and CAL11926 from the Multimission Archive at Space Telescope (MAST) and processed it with the IRAF/STSDAS pipeline program calwf3. Earlier data sets obtained during SMOV and reported in Kalirai et al. (2009) were all reprocessed with the updated calwf3 pipeline (version 2.0) and a common set of calibration files. All of the analysis presented here includes the new WFC3/IR flat field, based on on-orbit measurements (previous analysis still used the ground flat).

Most of the observations use the 128 pixel subarray on WFC3/IR, although we also obtained data using the 64 pixel, 256 pixel, and 512 pixel subarrays as well as a few full frame images (see Figure 1). In filters with the highest throughput, the full frame exposures often reach saturation after just 1 or 2 reads, making these data less useful for our present goals of accurate photometric characterization of the instrument (e.g., they have a poor up-the-ramp fit to the flux and can also be affected by cosmic rays). For the smallest 64 pixel subarray, the projection on the sky across the entire field is only 8.3 arcseconds and so a few exposures placed the star too close to the edge of the field to build a large aperture. In rare cases such as these, or occasionally where the star landed on a bad pixel, we ignored the data.

Our exposure times were typically set to just a few seconds to ensure a very high signal-to-noise (e.g., >100) detection of the star in the wide band filters. We used the RAPID readout sequence for this. For the medium and narrow-band filters, we used a mix of RAPID and SPARS10 readout sequences with exposure times varying from a few seconds to a few tens of seconds to ensure an accurate measurement. Almost all observations involved at least two dithered positions in each filter, occasionally including three or four dithered exposures. The dithers were typically a few pixels so all observations in both programs place the star near the center of the IR array.

We performed all of our analysis on calwf3 processed `_flt` images, multiplied by the pixel area map (available at <http://www.stsci.edu/hst/wfc3> – see Kalirai et al. 2010a). The pixel area map is actually not essential for this analysis since we are only interested in a relative measurement and the star is roughly at the same position of the detector in all exposures. We also tested the difference between measured photometry on multidrizzled `_drz` images compared to our `_flt` images on a subset of the data, and found that the two agree to within a small fraction of a percent.

Aperture photometry of the spectrophotometric standards on all images was performed with the standalone version of DAOPHOT (Stetson 1987; 1994), in a set of 12 apertures with radii ranging from 0.10 to 2.00 arcseconds. The sky was measured as the modal value in an annulus extending from 2.6 to 5.2 arcseconds. We find that our photometric comparisons of temporal stability are similar for different aperture choices, so we select $R = 3$ pixels (0.4 arcseconds) as the default aperture in the plots and analysis that follows. In fact, a slightly larger aperture yields the best standard deviations.

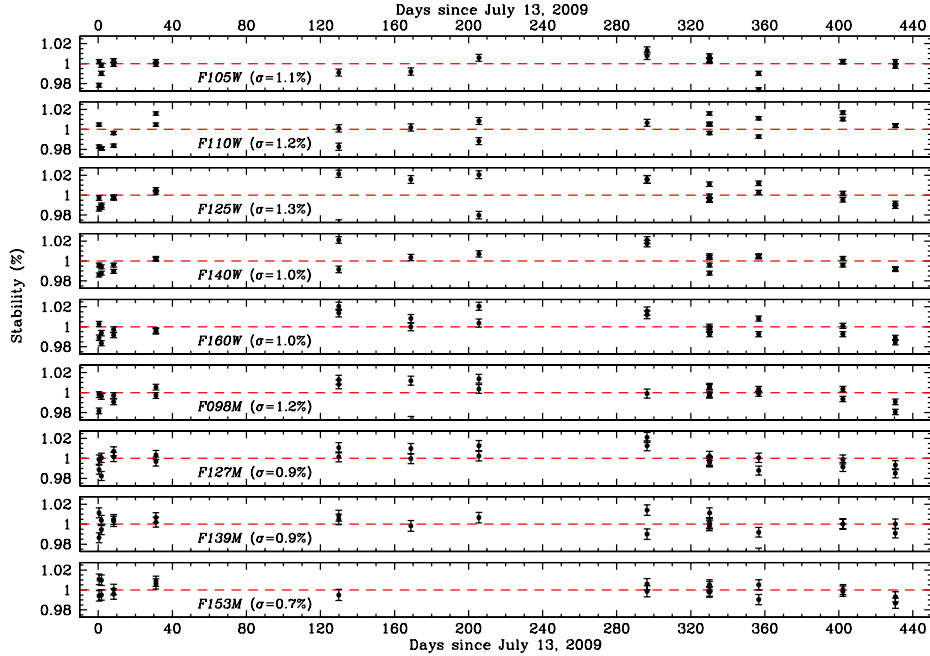


Fig. 2.— The temporal stability of WFC3/IR as measured from high signal-to-noise observations of the bright HST spectrophotometric standard P330E in all IR wide and medium-band filters (separate panels). At each of the epochs, measurements at all dither positions are shown as individual points. Over the entire time period extending from July 2009 to November 2010, the scatter is measured to be small (note the large tick marks denote $\pm 2\%$ variations). The formal standard deviation among all of these points is measured to be $\sim 1\%$ in each filter, with much better values for the subset of observations taken after day 280 which place the standard at approximately the same pixel, same readout, and a large number of samples (e.g., $\sigma = 0.5 - 1.0\%$ – see Section 4).

4. Measuring WFC3/IR’s Temporal Stability

The observations summarized in Table 1 almost completely span the time that WFC3 has been in orbit, and are well sampled throughout that period. The first images for P330E and GD 153 were obtained in July 2009 and the latest epoch considered in this analysis is from November 2010. We define the mean brightness of each of the standards for all observations in any given filter, and illustrate the scatter and measured standard deviation in six plots. Figures 2 and 3 show the results for the Solar analog P330E, where the first plot shows the wide and medium-band filters and the second plot shows the narrow-band filters. Similarly, the scatter for GD 153 is shown in Figures 4 and 5 and GD 71 is shown in Figures 6 and 7. For G191B2B, our data set only has two epochs and so the scatter is not yet well defined. In each panel, data from dithered observations are *not* averaged together and rather shown as individual measurements.

P330E WFC3/IR

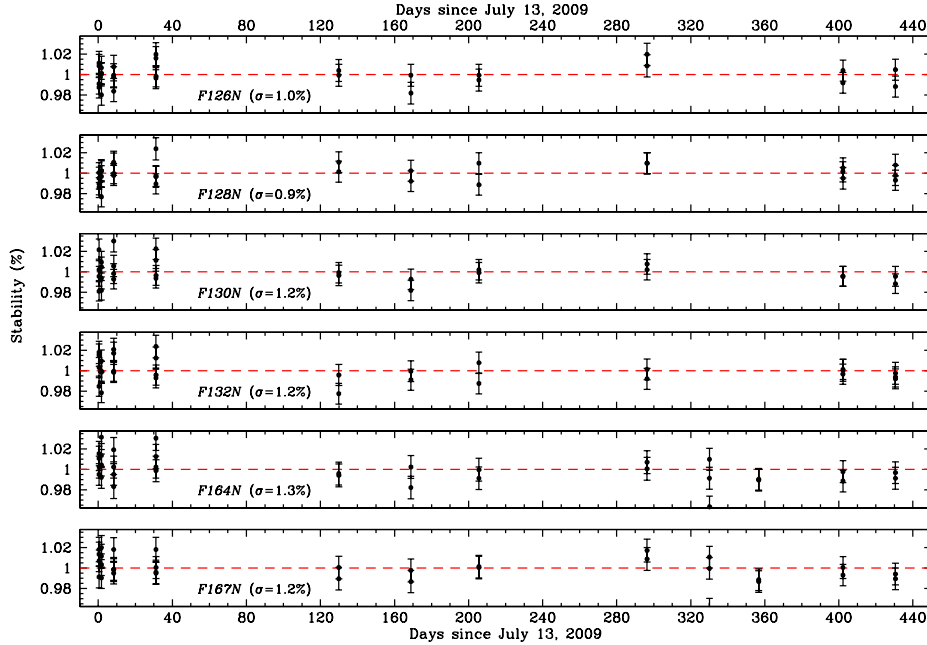


Fig. 3.— The temporal stability of WFC3/IR, as characterized from observations of P330E in the six narrow band filters. Given the larger uncertainties in these measurements, the vertical scale is made slightly larger than for Figure 2. The variations in the independent observations over the long time baseline are $\sim 1\%$, again indicating temporal stability to 99%.

Figure 2 demonstrates the scatter in our medium and wide-band filter observations of P330E. The large tick marks on each panel represent just $\pm 2\%$ variations, and the data fall within these bounds for all observations (excluding a few measurements for reasons outlined earlier). The formal standard deviation for each filter is listed on the plot and is $\sim 1\%$ over the full time baseline. If we restrict our comparison to just those data taken after day 280 (when the standard was placed on approximately the same pixel, and we used the same readout mode for all observations), the standard deviations for many of the filters are 0.5 – 1.0%. These recent observations were intentionally constructed to ensure that the star lands on approximately the same pixel and was observed with the same subarray and a large number of samples in the readout. These measurements therefore indicate that photometry of point sources with WFC3/IR is temporally stable to $>99\%$ over the first year of science operation. Figure 3 demonstrates the same measurements for P330E observed in narrow-band filters. Although the uncertainties are larger, these plots also demonstrate temporal stability to 99%.

Figures 4 and 5 demonstrate the scatter in the observations of the hot white dwarf standard GD 153. The uncertainties in these data are slightly larger than for P330E, but the same stability conclusions are confirmed. Figures 6 and 7 show the data for the hot white dwarf standard GD 71

GD153 WFC3/IR

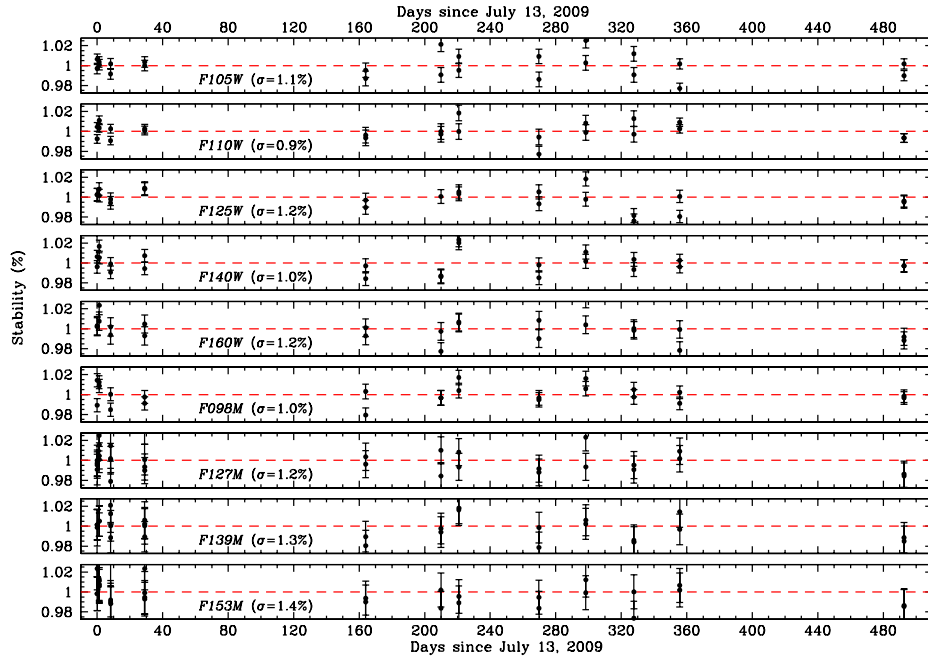


Fig. 4.— Same as Figure 2 for the wide and medium-band filters, but for GD 153.

GD153 WFC3/IR

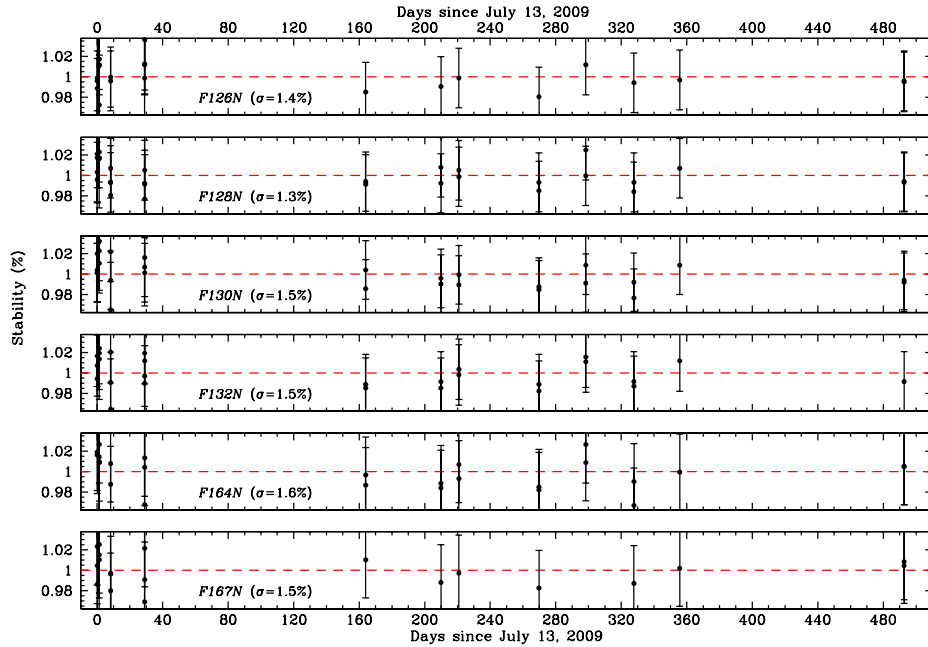


Fig. 5.— Same as Figure 3 for the wide and medium-band filters, but for GD 153.

GD71 WFC3/IR

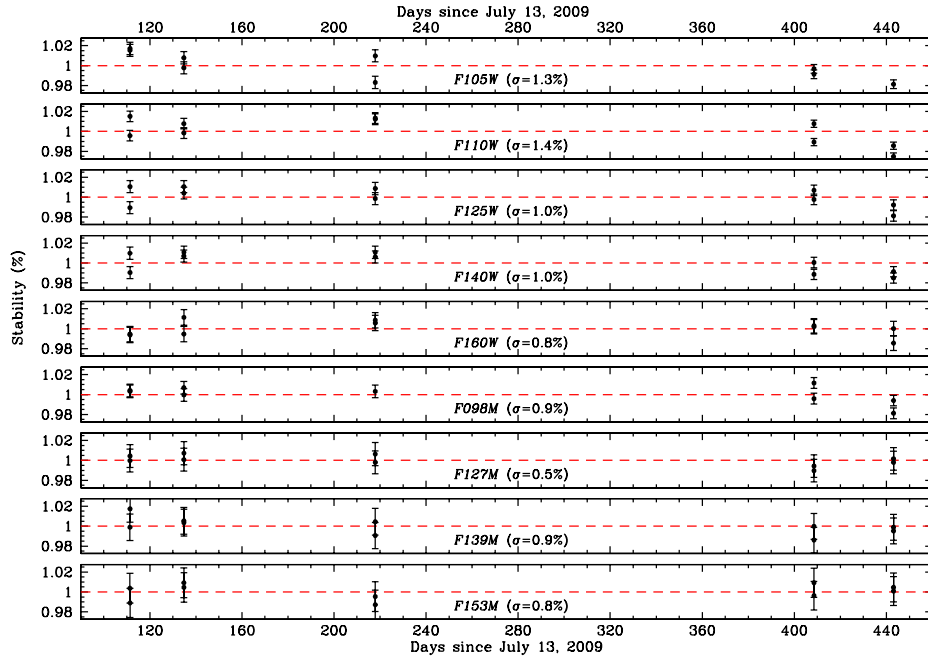


Fig. 6.— Same as Figure 2 for the wide and medium-band filters, but for GD 71.

GD71 WFC3/IR

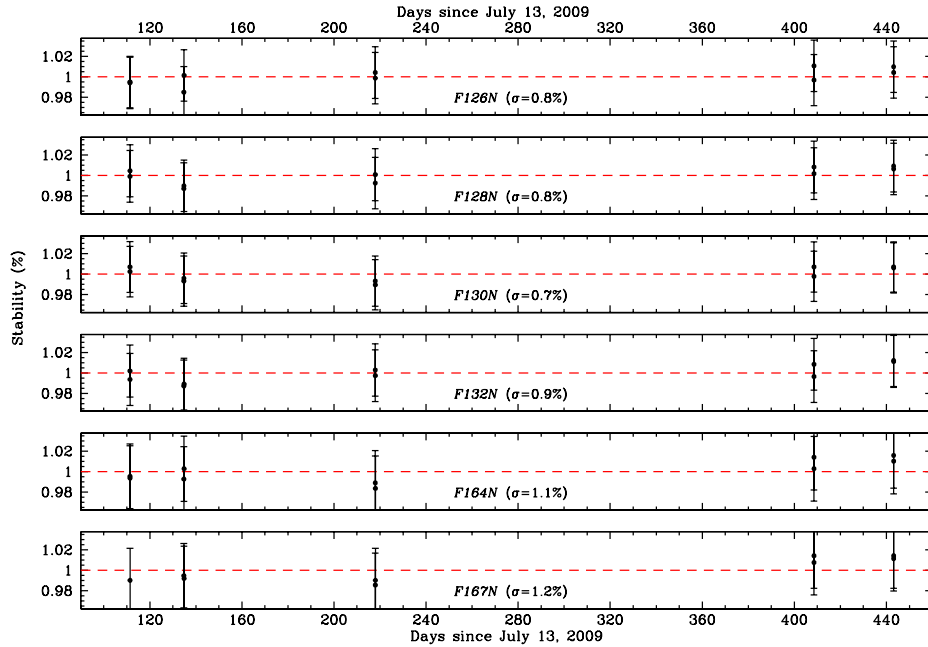


Fig. 7.— Same as Figure 3 for the wide and medium-band filters, but for GD 71.

over 5 epochs, and again the best observations show temporal stability to $>99\%$. For G191B2B, our sampling consists of just two epochs for the wide and medium-band filters separated by seven months, and the measurements at these two times are consistent with one another to within 1%. For the narrow-band filter observations of G191B2B, we currently have only one epoch of measurements.

5. Conclusions

We analyze more than 1200 individual high signal-to-noise observations of bright HST spectrophotometric standard stars to establish the temporal stability of WFC3/IR over its first 1.5 years of science operations. The data set consists of multiple dithered exposures in the 64, 128, 256, and 512 pixel subarrays as well as full frame images. Our analysis shows that the scatter among repeat measurements of the same star is small, with a formal standard deviation indicating that WFC3/IR is temporally stable to $>99\%$.

As reported in Kalirai et al. (2010b), the UVIS camera of WFC3 is also temporally stable to $>99.5\%$ over a similar baseline. In future cycles, spot check measurements of standard stars on both cameras should suffice in confirming their stable nature.

The 0.5 – 1.0% stability variation limits established for both instruments apply to standard point source photometry which is affected by both pixel-to-pixel variations in the flat field as well as inter-pixel sensitivity variations. Improvements in the characterization and calibration of these effects may allow the point source stability to improve.

References

- Anderson, J., & Bedin, L. R. 2010, *PASP*, 122, 1035
- Kalirai, J., et al. 2009, WFC3 ISR 2009-30 (CAL11451), “WFC3 SMOV Proposal 11451: The Photometric Performance and Calibration of WFC3/IR”
- Kalirai, J., et al. 2010a, WFC3 ISR 2010-08, “WFC3 Pixel Area Maps”
- Kalirai, J., et al. 2010b, WFC3 ISR 2010-14, “The Photometric Performance of WFC3/UVIS: Temporal Stability Through Year 1”
- Stetson, P. B. 1987, *PASP*, 99, 191
- Stetson, P. B. 1994, *PASP*, 106, 250